



J. Serb. Chem. Soc. 86 (5) 483–494 (2021)
JSCS–5436

The spectral study of azo dye and cationic surfactant interaction in ethanol–water mixture

NEELAM SHAHI¹, SUJIT KUMAR SHAH¹, AMAR PRASAD YADAV²
and AJAYA BHATTARAI^{1*}

¹Department of Chemistry, M.M.A.M.C., Tribhuvan University, Biratnagar, Nepal and

²Central Department of Chemistry, Tribhuvan University, Kirtipur, Nepal

(Received 16 November 2020, revised 10 March, accepted 11 March 2021)

Abstract: The interaction of the azo dye methyl red (MR) with dodecyl trimethyl ammonium bromide (DTAB) has been studied by the spectrometric methods through the azo-hydrazone tautomeric behaviour of MR for a series of the ethanol–water system (0.1, 0.2, 0.3 and 0.4 volume fractions of ethanol) at room temperature. The critical micelle concentration was determined using the conductometric technique with the increased ethanol volume, influenced by the solvent polarity and the architectural flexibility of methyl red. The azo form of methyl red brings the electrostatic interaction with the cationic surfactant through the adsorption phenomenon. The binding parameters were calculated with the aid of a modified Benesi–Hildebrand equation.

Keywords: molar absorptivity; binding constant; standard Gibbs energy.

INTRODUCTION

The performance of the interaction between dye and surfactant is one of the basic requirements for understanding the dyeing process and textile finishing.^{1–5} In order to study this process numerous researches have been performed by the selective research techniques to access the basic information of the interactions for the process of the molecular complex formation in the dye-surfactant ion pair.^{6–11}

There are no specified studies about the azo dye methyl red with cationic surfactant dodecyl trimethyl ammonium bromide, using various methods.^{12–17} The absorbance peak of methyl red was decreased, due to the photodegradation in water. It was checked after 10, 20 and 35 min (complete photodegradation) by the kinetic analysis treatment, which is based on the azo dye photosensitization.¹⁸ The anchoring position of the –COOH group at the para position of methyl red tuned the wavelength and intensity¹⁹ and showed a broad peak at 519 nm in

*Corresponding author. E-mail: bkajaya@yahoo.com
<https://doi.org/10.2298/JSC201116020S>

hydrazone form, indicating the considerable optical nonlinearities.²⁰ The visible spectrum of MR in aqueous solutions is marked by the overlap of a principal peak at 520 ± 15 nm and a shoulder peak at 435 ± 20 nm, for the hydroazo (acidic) and the azo (alkaline) species respectively.²¹

In this paper, the spectrophotometric study of the interaction between azo dye methyl red (MR) (Fig. 1) and cationic surfactant dodecyl trimethyl ammonium bromide (DTAB) (Fig. 2) is described.

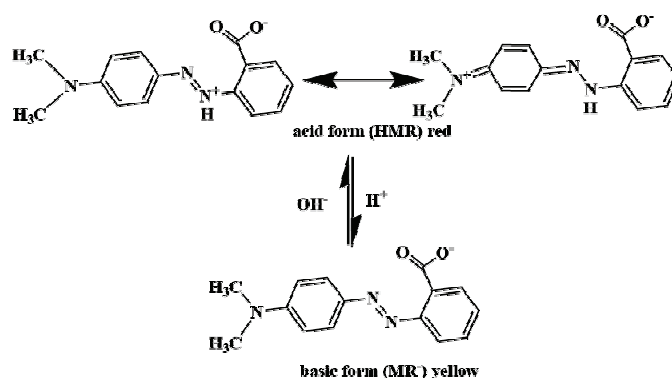


Fig. 1. Acid and basic forms of methyl red.

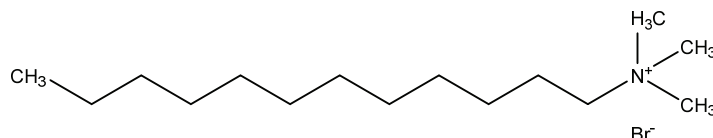


Fig. 2. Dodecyl trimethyl ammonium bromide.

The interaction between dye and surfactant plays an important role in the formation of the complex as shown in Fig. 3.

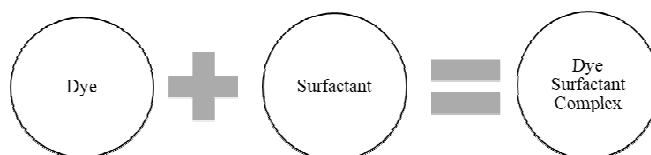


Fig. 3. The interaction between dye and surfactant for their complex formation.

To study the significance of the interaction of the molecular complex formation of the azo dye–cationic surfactant ion pair, the absorbance measurement was performed for the series of the ethanol–water systems containing the various volumes of ethanol (0.1, 0.2, 0.3 and 0.4 volume fractions of ethanol). A modified model was applied in order to determine the binding constants and the change of standard Gibbs energy of binding for the molecular complex formation

of the ion pair. The result displayed the influence of volume fraction of ethanol on the formation of dye–surfactant molecular complex and the importance of the interaction of azo dye and cationic surfactant.

Methyl red is a good example which illustrates that both the linear and non-linear optical properties can be seen through the absorbance technique. The literature shows the azo-hydrazone tautomerism of MR, with the change of surfactant charge effects and without the change in solvent polarity, generates the azo-hydrazone tautomerism as shown in Fig. 1.^{14,20,21} The optical sensitivity of azo dye makes the interaction study interesting with a cationic surfactant.¹⁴ The interaction of the azo dye and the cationic surfactant brings the flexibility in absorbance which alters the nature of spectra.^{12,13}

The present study describes the azo-hydrazone tautomerism, using the absorbance techniques along with the observation of binding constant and the change of Gibbs energy of binding of DTAB on MR, which will facilitate the advancement in the molecular design of similar derivatives, specifically a –COOH group azo dye through the photosensitized system in optical tenability. We applied a spectrophotometric technique and used the modified Benesi-Hildebrand equation in order to calculate the binding constant of methyl red, in the presence of DTAB/ethanol/water system. Such a concept was applied to calculate the binding parameters (the binding constant and the change of standard Gibbs energy of binding) for dyes (methylene blue and methyl orange) absorbance in DTAB–SDS mixed surfactant, by the absorption technique in an aqueous medium, without using critical micelle concentration (*CMC*) values.²²

EXPERIMENTAL

Chemicals

DTAB and MR were obtained from Loba Chemicals, India. Similarly, MR (95 %) was purchased from Ranbaxy, India, and used without purification and spectroscopy quality ethanol was obtained from Merck, India.

Preparation of solutions

Four types of solutions were prepared to study the interaction of MR–DTAB in the ethanol–water system.

In the first part of the study, 0.1, 0.2, 0.3 and 0.4 volume fractions of ethanol–water mixed solvent were prepared. Sequentially the surfactant (DTAB, concentration ranging from 10^{-4} to 0.12 mol L^{-1} and the azo dye MR at a constant concentration of $2.97 \times 10^{-4} \text{ mol L}^{-1}$ were prepared separately in the respective volume fraction of ethanol–water. In the second part of the study, the spectral absorbance corresponding to wavelengths ranging from 300 to 700 nm of the solution at variable concentrations of DTAB, with a constant dye concentration of MR, was obtained for the interaction study.

Methods

The spectrophotometric measurements were recorded by a single beam microprocessor UV–Vis spectrophotometer (LT-290 Model, India) from which UV–Vis spectra were registered at room temperature using 1 cm length quartz cuvette. The conductometric measure-

ments were performed in order to obtain the *CMC* value of DTAB in the absence, as well as the presence of MR at 0.1, 0.2, 0.3 and 0.4 volume fraction of ethanol, as described in the literature.

RESULTS AND DISCUSSION

UV – Vis spectra of azo dye in ethanol – water mixture

The UV–Vis spectra of MR in the ethanol-water mixture (from 0.1 to 0.4 volume fractions of ethanol) were measured at the constant dye concentration ($C_{\text{dye}} = 2.97 \times 10^{-4} \text{ mol/L}^{-1}$). When the graph displaying the relation between absorbance (A) and wavelength (λ) was plotted (Fig. 4) the redshift was observed, from 0.4 to 0.2 volume fraction of ethanol, which was due to an increase in the dielectric constant and the reduction of solubility.²³ But the redshift between 0.1 and 0.2 volume fraction of ethanol were not observed. The absorbance spectra of MR at 0.1 volume fraction of ethanol showed two broad peaks at λ_{abs} of 532 and 529 nm. However, the absorbance spectra of MR showed a slight redshift with broad peaks at λ_{abs} of 528, 529 and 532 nm for 0.4, 0.3 and 0.2 volume fraction of ethanol, respectively. The observed peaks of MR as hydrazone (acidic) species were found at 0.1, 0.2, 0.3 and 0.4 volume fraction of ethanol. Thus, the UV–Vis spectra of methyl red were found to be solvent-dependent and the absorbance of methyl red in 0.4 volume fraction of ethanol is largest among 0.3, 0.2, 0.1 volume fraction of ethanol (Table I).

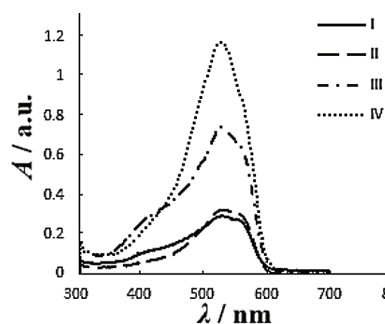


Fig. 4. Visible spectra of MR at various volume fractions of ethanol. Here, I, II, III and IV represent volume fraction of ethanol: 0.1, 0.2, 0.3 and 0.4, respectively.

TABLE I. The calculation for ϵ_0 from Eq. (4)

Volume fraction of ethanol	$\lambda_{\text{max}} / \text{nm}$	$A / \text{a. u.}$	$\epsilon_0 / \text{L mol}^{-1}\text{cm}^{-1}$
0.1	532	0.2938	989.22
0.2	532	0.3268	1100.34
0.3	529	0.7428	2501.01
0.4	528	1.1798	3972.39

UV – Vis spectra of cationic surfactant – azo dye interactions in ethanol – water mixture

The UV–Vis spectra of MR in ethanol–water–DTAB were observed at constant dye concentration. When the graph (Fig. 5) was plotted (absorbance vs. wavelength), the absorbance peak of MR in ethanol–water–DTAB showed a broad absorbance peak at λ_{abs} of 419, 424, 421 and 420 nm for 0.1, 0.2, 0.3 and 0.4 volume fraction of ethanol, respectively. The peak range is attributed to the azo form of MR within ethanol–water–DTAB. The blue shift is observed for the constant dye concentration at the variable concentration of DTAB for the spectra of 'V' of legend represented in Fig. 5 – A, B, C and D were due to the formation of H-aggregates during the electrostatic interaction in the molecular complex (Fig. 3).²⁴

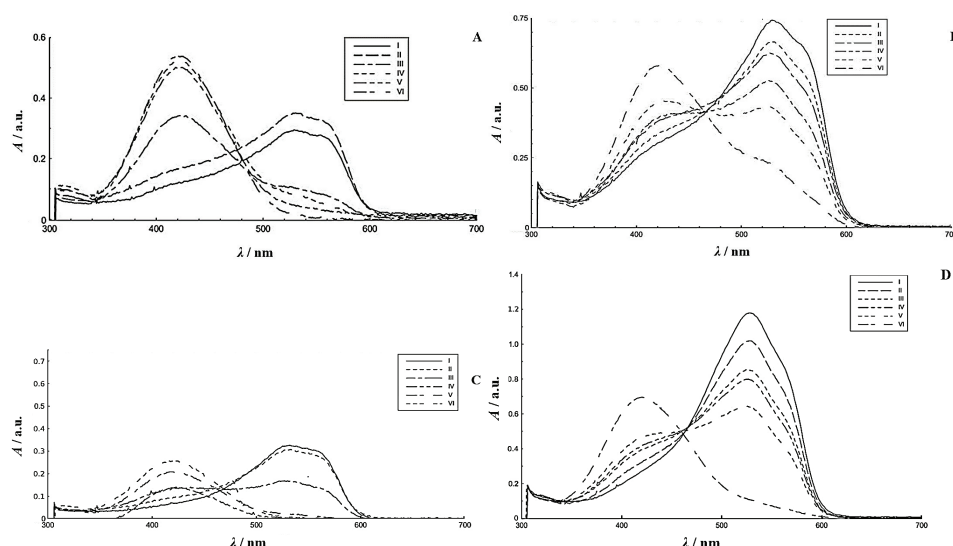


Fig. 5. Absorption spectra for methyl- red with presence and absence of DTAB; volume fraction of ethanol: 0.1 (A); 0.2 (B); 0.3 (C); 0.4 (D).

In the recent study, the interaction of CTAB (cationic surfactant) with MR is attributed to the azo form at λ_{abs} of 414 nm, whereas the interaction of AOT (anionic surfactant) with MR is subjected to the hydrazone form at $\lambda_{\text{abs}} = 519$ nm.¹⁴

In the present work, the interaction of cationic surfactant (DTAB) with the azo dye (MR) is studied through the spectrophotometric method. In the case of MR, due to its photoisomerisation, its azo(basic) form attracts the ionized surface-active agents. The ionic surfactants dissociate as electrolytes (weak or strong) which shows the adsorption phenomenon. The idealized charged spherical micelles are partially neutralized by the counterions forming the stern layer as shown in Fig. 6. The long alkyl groups of surfactants are in the interior of the micelle and the hydrophilic (polar) part of surfactants are at the surface, which exhibits the electrostatic interaction with the counterions of azo dye. Due to such

interactions, approximately 60–80 % micellized charge is neutralized by counterions and the remaining unbounded counterions are moving freely, forming the Gouy–Chapman double layer.

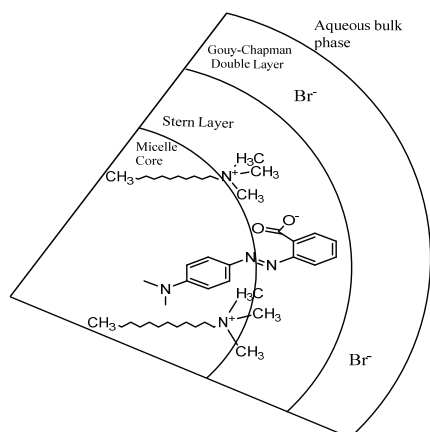


Fig. 6. A schematic structure of cationic surfactant with azo dye.²⁷

We observed the interaction through different spectral behaviour and the obtained absorbance concerning the constant concentration of azo dye in the absence and the presence of a variable concentration of DTAB, for the series of the ethanol–water mixture, at room temperature.²⁵

The spectral characteristics of azo dye were greatly influenced by the addition of cationic surfactant in the presence of various ethanol concentrations. The absorbance was increased with rised ethanol volume (Fig. 4), which contributes to the formation of molecular complex between the cationic surfactant and the azo dye as presented in Fig. 6. The origin of electrostatic interaction on the hydrocarbon core of the surfactant, at constant dye concentration, was analysed due to a decrease in absorbance with a higher concentration range of ionic surfactant.²⁶

Various natures of absorption spectra of a dye with the presence and absence of cationic surfactant had been observed for the series of the ethanol–water mixtures as shown in Fig. 5.

Absorption spectra in Fig. 5A. In 0.1 volume fraction of ethanol, as the concentration of DTAB increased the MR band intensity initially increased and finally decreased. Here, I, II, III, IV, V and VI represents the DTAB concentrations ($C/\text{mol L}^{-1}$), which were varied from as 0, 0.011695, 0.023390, 0.035085, 0.046780 and 0.116951, respectively.

The absorption spectra in Fig. 5B. In 0.2 volume fraction of ethanol, as the concentration of DTAB increased the MR band intensity initially decreased and then increased. Here, I, II, III, IV, V and VI represents the DTAB concentrations

($C/\text{mol L}^{-1}$), which were varied from as 0, 0.0105994, 0.0211988, 0.0317982, 0.0423976 and 0.1059940, respectively.

The absorption spectra in Fig. 5C and D. In 0.3 and 0.4 volume fraction of ethanol, as the concentration of DTAB increased the MR band intensity decreased. Here, in the case of Fig 5C, I, II, III, IV, V and VI represent DTAB concentrations ($C/\text{mol L}^{-1}$), which were varied as 0, 0.011122, 0.022244, 0.033366, 0.044488 and 0.111220, respectively. In the case of Fig 5D, I, II, III, IV, V and VI represent DTAB concentrations ($C/\text{mol L}^{-1}$), which were varied as 0, 0.011122, 0.022244, 0.033366, 0.044488 and 0.111220, respectively.

Analysis of cationic surfactant – azo dye interactions in ethanol – water mixture

We used the spectrophotometric technique and confirmed the surfactant induced spectral change by binding and thermodynamic properties, evaluated through the spectral changes, as the observed absorbance at different surfactant concentrations at constant dye concentration in the ethanol-water mixture, Fig. 5.

Shah *et al.*²⁸ investigated the CMC of DTAB in the ethanol–water mixture up to 0.6 volume fraction of ethanol using conductometry and tensiometry. The CMC was found to be increased up to 0.4 volume fraction of ethanol due to a decrease in hydrophobic character, with the addition of ethanol and the decrease in CMC up to 0.6 due to entrance of alcohol molecules into a micellar core. We used the conductometry technique to obtain the CMC value of DTAB in the absence, as well as in the presence of MR, at 0.1, 0.2, 0.3 and 0.4 volume fraction of ethanol. The sequential increased CMC is obtained in the adopted system, but the CMC values are suppressed with MR, in comparison to CMC values in the absence of MR.^{28,29} The decreased CMCs of DTAB, in the presence of MR is due to the change in the status of the molecular complex system.²⁹ The CMC values are listed the in Table II along with literature.²⁸

TABLE II. CMC values of DTAB in the presence and absence of MR at 298.15 K

Volume fraction of ethanol	CMC / mol L ⁻¹		
	With MR	Without MR	Without MR ²⁸
0.1	0.01497	0.01637	0.0151
0.2	0.02102	0.02178	0.0214
0.3	0.02110	0.03054	0.0325
0.4	0.02487	0.04375	0.0462

It can be seen that both the conductivity and CMC of DTAB decrease with the addition of MR, as it is presented in Fig. 7, with is in agreement with the literature.³⁰

The interaction between the dye and micellized surfactant can be described by the Eq. (1). Here, the term D, S, DS and K_b represent the dye, surfactant, dye–surfactant associate and binding constant, respectively:



Fig. 8 displays for the interaction study for the determination of the binding constant (K_b), related to the scheme on Fig. 6, which is calculated using the modified Benesi–Hildebrand Equation (2):²²

$$\frac{D_T}{\Delta A} = \frac{1}{(\epsilon_m - \epsilon_0)} + \frac{1}{K_b(\epsilon_m - \epsilon_0)C_s} \quad (2)$$

$$\Delta A = A - A_0 \quad (3)$$

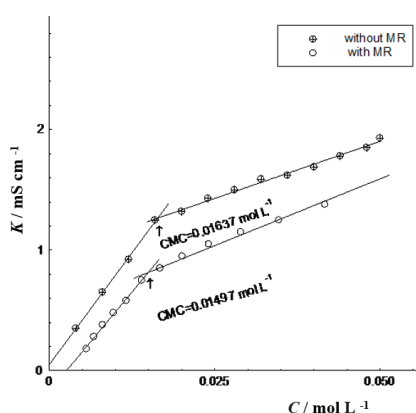


Fig. 7. Conductivity *versus* concentration of DTAB at 0.1 volume fraction of ethanol with and without MR.

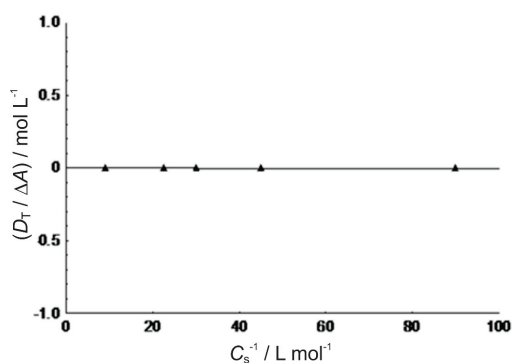


Fig. 8. The plot of $(D_T/\Delta A)$ against reciprocal of C_s for MR with DTAB at 0.3 volume fraction of ethanol. Here, $y = 3.19 \times 10^{-5}x - 8.54 \times 10^{-4}$; Max. dev. 6.05×10^{-9} , $r^2 = 1.00$.

The term D_T in Eq. (2) and A in Eq. (3) represents the concentration and the absorbance of dye. The left side of Eq. (2) consists of ΔA , which is the difference between the absorbance of dye in the presence and the absence of DTAB is expressed in Eq. (3). The right side of Eq. (2) consists of term ϵ_m , ϵ_0 , C_s and K_b which represents the molar absorptivity of the dye, the molar absorptivity of dye fully bound to micelles, the concentration of DTAB (surfactant) and the binding constant respectively. Eq. (2) can be applied for studying spectral behaviour containing *CMC* value,²⁹ or without *CMC* value.²² The molar absorptivity of dye

represented as ϵ_0 was calculated using the relation the rearranged Beer–Lambert Equation (4):

$$\epsilon_0 = \frac{A}{LC} \quad (4)$$

The Eq. (4) term consists of terms A , L and C , which represents the absorbance for a given wavelength, the length of cuvette and the concentration of dye, respectively.

The maximum wavelength corresponding to absorbance (λ_{\max} / nm), absorbance for a given wavelength (A / a.u.), length of the cuvette (L / cm), the concentration of dye (D_T / mol L⁻¹), and molar absorptivity of dye (ϵ_0 / L mol⁻¹ cm⁻¹) are the values and its interactive relationship are represented in Table I. Here, $L = 1$ cm, $C = 2.97 \times 10^{-4}$ mol L⁻¹. It can be seen that the highest molar absorptivity of azo dye at 0.4 volume fraction of ethanol is due to the influence of a higher volume of ethanol in water.²⁴

The binding constant (K_b) can be determined by plotting ($D_T/\Delta A$) against reciprocal of C_s for DTAB, with MR at 0.3 volume fraction of ethanol, as shown in Fig. 8, as a typical example. From the slope and the intercept, the binding constant was calculated at a different volume fractions of ethanol and tabulated in Table III.

TABLE III. Calculation of the slope, intercept and binding constant in the different volume fractions of ethanol

Volume fraction of ethanol	Slope $\times 10^5$	Intercept $\times 10^4$	K_b / L mol ⁻¹
0.1	6.22	7.59	12.2
0.2	1.3.3	6.48	4.87
0.3	3.19	8.54	26.77
0.4	1.48	2.96	20.00

Table III shows that the binding values, which were highest at the volume fraction of ethanol is 0.3, increased which is because the hydrophilic head portion of surfactants plays a significant role in dye-surfactant interaction.³¹ When the volume of ethanol is 0.2, the binding value between the azo dye and the surfactant is lowest, due to the abnormal aggregation around the hydrophilic portion of DTAB micelles by MR molecules.

Many researchers had reported that the addition of mixed solvent completely blocks the micellization behaviour of surfactant at a certain concentration level of mixed solvent.²⁹

The thermodynamic parameter, the change of standard Gibbs energy of binding can be obtained using Eq. (5):

$$\Delta G^\ominus = -RT \ln K_b \quad (5)$$

In Eq. (5), the left side represents the change of standard Gibbs energy of binding, ΔG^\ominus , whereas, on the right side, R represents a universal gas constant, the recorded room temperature of the laboratory is denoted by T and K_b is the binding constant. The values are presented in Table IV, which indicates the interaction between the dye and ionic surfactant, at 0.1, 0.2, 0.3 and 0.4 volume fractions. This is due to the strong electrostatic interaction between the hydrophilic cationic head of surfactant and azo dye as well as with a decrease in the dielectric constant with the addition of mixed solvent.^{30,32}

TABLE IV. Calculation of ΔG^\ominus in the different volume fractions of ethanol

Volum fraction of ethanol	$\Delta G^\ominus / \text{kJ mol}^{-1}$
0.1	-6010.31
0.2	-3803.77
0.3	-7898.50
0.4	-7197.98

CONCLUSION

Based on the spectral study of the interaction between the azo dye MR and the cationic surfactant DTAB, the following conclusions can be summarized.

The spectrophotometric technique is the best method for the study of the dye–surfactant interaction, by a wide range of spectral analysis, with typical azo-hydrazone tautomerism in the ethanol–water mixture. The variable absorbance values ultimately indicated the scheme of dye–surfactant interaction through the adsorption phenomena and the formation of a dye surfactant complex. The interaction behaviour was studied through thermodynamic processes, which were characterized by the variable binding constant and the change of standard Gibbs energy of binding. The mixed solvent media containing alcohol–water mixtures broke down the structure of water, which lowered down the dielectric constant and hence *CMC* of DTAB increases, with the addition of ethanol in water, while *CMC* values of DTAB decrease with the presence of methyl red.

Acknowledgement. This work was supported by the University Grants Commission, Sanothimi, Bhaktapur, Nepal, under the funding award no. PhD-75/76-S&T-05.

ИЗВОД

СПЕКТРОСКОПСКО ИСПИТИВАЊЕ ИНТЕРАКЦИЈЕ АЗО БОЈЕ И КАТЈОНСКОГ СУРФАКТАНТА У СМЕШИ ЕТАНОЛ–ВОДА

NEELAM SHAH¹, SUJIT KUMAR SHAH¹, AMAR PRASAD YADAV² и AJAYA BHATTARAI¹

¹Department of Chemistry, M.M.A.M.C., Tribhuvan University, Biratnagar, Nepal и ²Central Department of Chemistry, Tribhuvan University, Kirtipur, Nepal

Интеракција азо боје метил-црвена (MR) и додецилтриметиламонијум-бромида (DTAB) је спектроскопски испитивана праћењем азо-хидразон таутомерног понашања MR за серију смеша етанол–вода (запреминске фракције етанола: 0,1, 0,2, 0,3 и 0,4) на собној температури. Критична мицеларна концентрација је одређивана кондуктометријски, и

са повећањем запремине етанола на њу утиче поларност растварача и структурна флексибилност MR. Азо облик MR се адсорбује на сурфактанту електростатичким интеракцијама. Параметри везивања су израчунати применом Бенеси–Хилдебранд (Benesi–Hildebrand) једначине.

(Примљено 16. новембра 2020, ревидирано 10 марта, прихваћено 11. марта 2021)

REFERENCES

1. G. Kyzas, E. Peleka, E. Deliyanni, *Materials* **6** (2013) 184 (<https://doi.org/10.3390/ma6010184>)
2. A. Bhattarai, A. K. Yadav, S. K. Sah, A. Deo, *J. Mol. Liq.* **242** (2017) 831 (<https://doi.org/10.1016/j.molliq.2017.07.085>)
3. A. Pal, A. Garain, D. Chowdhury, M. H. Mondal, B. Saha, *Tenside Surf. Det.* **57** (2020) 401 (<https://doi.org/10.3139/113.110700>)
4. S. Tunç, O. Duman, B. Kancı, *Dyes Pigments* **94** (2012) 233 (<https://doi.org/10.1016/j.dyepig.2012.01.016>)
5. K. M. Sachin, S. A. Karpe, M. Singh, A. Bhattarai, *Roy. Soc. Open Sci.* **6** (2019) 181979 (<https://doi.org/10.1098/rsos.181979>)
6. S. Fazeli, B. Sohrabi, A. R. Tehrani-Bagha, *Dyes Pigments* **95** (2012) 768 (<https://doi.org/10.1016/j.dyepig.2012.03.022>)
7. H. Akbaş, Ç. Kartal, *Spectrochim. Acta, A* **61** (2005) 961 (<https://doi.org/10.1016/j.saa.2004.05.025>)
8. S. Malik, A. Ghosh, P. Sar, M. H. Mondal, K. Mahali, B. Saha, *J. Chem. Sci.* **129** (2017) 637 (<https://doi.org/10.1007/s12039-017-1276-4>)
9. M. F. Nazar, S. S. Shah, M. A. Khosa, *J. Surfact. Deterg.* **13** (2010) 529 (<https://doi.org/10.1007/s11743-009-1177-8>)
10. M. H. Mondal, S. Malik, B. Saha, *Tenside Surf. Det.* **54** (2017) 378 (<https://doi.org/10.3139/113.110519>)
11. M. Mondal, M. Ali, A. Pal, B. Saha, *Tenside Surf. Det.* **56** (2019) 516 (<https://doi.org/10.3139/113.110654>)
12. S. Biswas, A. Pal, *Talanta* **206** (2020) 120238 (<https://doi.org/10.1016/j.talanta.2019.120238>)
13. F. Ahmadi, M. A. Daneshmehr, M. Rahimi, *Spectrochim. Acta, A* **67** (2007) 412 (<https://doi.org/10.1016/j.saa.2006.07.033>)
14. S. Sharifi, M. F. Nazar, F. Rakhshanizadeh, S. A. Sangsefedi, A. Azarpour, *Opt. Quantum Elec.* **52** (2020) (<https://doi.org/10.1007/s11082-020-2211-3>)
15. C. Hahn, A. Wokaun, *Langmuir* **13** (1997) 391 (<https://doi.org/10.1021/la9603378>)
16. S. Chanda, K. Ismail, *IJC A* **48** (2009) 775 (<http://nopr.niscair.res.in/handle/123456789/4686>)
17. M. H. Mondal, S. Malik, A. Roy, R. Saha, B. Saha, *RSC Adv.* **5** (2015) 92707 (<https://doi.org/10.1039/c5ra18462b>)
18. R. B. Narayan, R. Goutham, B. Srikanth, K. P. Gopinath, *J. Environ. Chem. Eng.* **6** (2018) 3640 (<https://doi.org/10.1016/j.jece.2016.12.004>)
19. L. Zhang, J. M. Cole, P. G. Waddell, K. S. Low, X. Liu, *ACS Sustain. Chem. Eng.* **1** (2013) 1440 (<https://doi.org/10.1021/sc400183t>)
20. D. N. Christodoulides, I. C. Khoo, G. J. Salamo, G. I. Stegeman, E. W. Van Stryland, *Adv. Opt. Photonics* **2** (2010) 60 (<https://doi.org/10.1364/aop.2.000060>)
21. M. R. Plutino, E. Guido, C. Colleoni, G. Rosace, *Sens. Actuators, B* **238** (2017) 281 (<https://doi.org/10.1016/j.snb.2016.07.050>)

22. K. M. Sachin, S. A. Karpe, M. Singh, A. Bhattarai, *Heliyon* **5** (2019) e01510 (<https://doi.org/10.1016/j.heliyon.2019.e01510>)
23. A. A. Rafati, S. Azizian, M. Chahardoli, *J. Mol. Liq.* **137** (2008) 80 (<https://doi.org/10.1016/j.molliq.2007.03.013>)
24. M. S. Ramadan, N. M. El-mallah, G. M. Nabil, M. Sherif, *J. Dispers. Sci. Technol.* **40** (2018) 1 (<https://doi.org/10.1080/01932691.2018.1496837>)
25. K. K. Karukstis, J. P. Litz, M. B. Garber, L. M. Angell, G. K. Korir, *Spectrochim. Acta, A* **75** (2010) 1354 (<https://doi.org/10.1016/j.saa.2009.12.087>)
26. M. L. Moyá, A. Rodríguez, M. del Mar Graciani, G. Fernández, *J. Colloid Interf. Sci.* **316** (2007) 787 (<https://doi.org/10.1016/j.jcis.2007.07.035>)
27. M. E. D. Garcia, A. Sanz-Medel, *Talanta* **33** (1986) 255 ([https://doi.org/10.1016/0039-9140\(86\)80060-1](https://doi.org/10.1016/0039-9140(86)80060-1))
28. S. K. Shah, S. K. Chatterjee, A. Bhattarai, *J. Mol. Liq.* **222** (2016) 906 (<https://doi.org/10.1016/j.molliq.2016.07.098>)
29. K. Edbey, A. El-Hashani, A. Benhmid, K. Ghwel, M. Benamer, *Chem. Sci. Int. J.* **24** (2018) 1 (<https://doi.org/10.9734/csji/2018/44312>)
30. P. Shah, N. Jha, A. Bhattarai, *J. Chem-Ny.* **2020** (2020) 5292385 (<https://doi.org/10.1155/2020/5292385>)
31. A. Rodríguez, M. del M. Graciani, M. L. Moyá, *Langmuir* **24** (2008) 12785 (<https://doi.org/10.1021/la802320s>)
32. S. Bračko, J. Špan, *Dyes Pigments* **50** (2001) 77 ([https://doi.org/10.1016/S0143-7208\(01\)00025-0](https://doi.org/10.1016/S0143-7208(01)00025-0)).